ELSEVIER

Journal of Power Sources 84 (1999) 187–193

JOURNAL OF POWER SOURCES

www.elsevier.com/locate/jpowsour

Methanol steam reforming in a fuel cell drive system

W. Wiese, B. Emonts, R. Peters *

Institut für Werkstoffe und Verfahren der Energietechnik (IWV-3), Forschungszentrum Jülich, D-52425 Jülich, Germany

Accepted 28 June 1999

Abstract

Within the framework of the Joule III project a *c*ompact *m*ethanol *r*eformer (CMR) with a specific weight of 2 kg/kW (lower heating value of H_2) was developed. This CMR contains a methanol and water vaporizer, a steam reformer, a heat carrier circuit and a catalytic burner unit. A laboratory fixed-bed reactor consisting of four tubes which could be filled with different amounts of catalyst was used to investigate the catalyst performance and the ageing behaviour. A hydrogen yield of 10 $m^3_N/(h\ l_{Cat})$ can be achieved at 280°C. In this case, the methanol conversion rate is 95% and the dry product gas contains 0.9% CO. A linear decrease of the catalyst activity was observed which can be described by a loss of active catalyst mass of 5.5 mg/h. The catalyst was operated for more than 1000 h without having exhibited activity losses that made a catalyst change necessary. Besides, the stationary behaviour of the reforming reactor, the dynamic behaviour was studied. The time needed for start-up procedures has to be improved for reformers of a next generation. Moreover, the hydrogen production during reformer load changes will be discussed. Simulations of the power train in driving cycles show the different states of a reformer during dynamic operation.

Keywords: Catalyst ageing; Compact methanol reformer; Dynamic operation; Fuel cell drive system; Simulation

1. Introduction

The interest in using new drive trains and to some extent alternative energy carriers for traction has increased in recent years due to serious discussions about air pollution, traffic and the quantity of energy resources [1–4]. Electric drive trains with batteries, internal combustion engines using natural gas or DME, and fuel cell drive systems [5,6] are of major interest in worldwide advanced development programs and demonstration projects. The efficiencies of such systems concerning both the power train and the energy conversion chain (full fuel cycle: FFC) are discussed together with the reduction potential for the related emissions by Höhlein et al. [7].

A fuel cell drive system based on methanol as the fuel consists of the following main components: a methanol steam reformer, a catalytic burner which provides the process heat for the reformer and converts all burnable gases in the flue gas into water and carbon dioxide, a gas cleaning unit which reduces the CO content of the hydrogen-rich gas and feeds the PEFC. Additionally, a gas storage system is necessary to feed the fuel cell during the start-up phase and in speed-up phases, when the gas generation system could not produce enough hydrogen. An overview of a fuel cell drive system is shown in Fig. 1 [8]. The advantages of such a system are the following.

1. The regulated emissions of CO, NO_x and unburnt hydrocarbon are reduced by a factor of up to 1000 compared to the ULEV standard. This has been discussed in more detail in a former publication [9].
2. Gas processing, especially the reforming process, is rather simple using methanol in comparison to the reforming of gasoline.
3. The usage of methanol as a liquid fuel avoids the problems concerning the on-board storage of hydrogen as an ideal fuel for the fuel cell.

Besides low emission behaviour and high energy efficiency, there are demands on the system concerning its performance.

1. The compact methanol reformer (CMR) should have a low specific weight of 1–2 kg/kW_{el}.
2. The useful operation time of the catalyst should be comparable to the operation time of an internal combustion engine. This leads to an operation time of about 4000 h and a lifetime of 10 years.
3. The demands on dynamic behaviour are rather high. Load changes should be performed in such a way that 30% of the original demand is fulfilled after 0.2 s.

* Corresponding author

0378-7753/99/$ - see front matter
PII: S0378-7753(99)00316-X

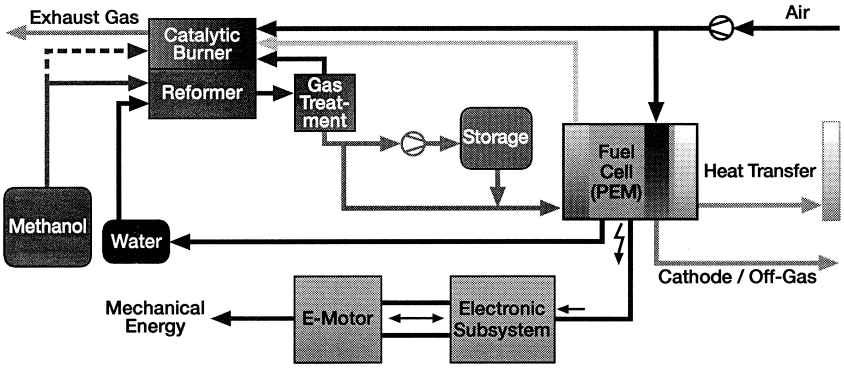

Fig. 1. Fuel cell drive system [8].

In previous works the general performance of a methanol steam reforming reactor is discussed [10] regarding the gas cleaning system [11,12] and the whole fuel conditioning process [4,12]. Aspects of catalyst ageing and its importance for the technical design of a methanol steam reformer are given by Düsterwald [13] and Düsterwald et al. [14].

In Sections 2–4, preliminary results from a reforming reactor will be presented and discussed. The performance and ageing behaviour of a reforming catalyst were investigated. Additionally, the dynamic behaviour was analyzed. Results from these experiments were integrated into simulations of the drive system in the New European Driving Cycle (NEDC). Demands on the components can be determined from the simulation results.

2. Experimental set-up

The experiments were carried out in a methanol steam reformer consisting of four reactor tubes that were individually balanced [13,14]. The set-up includes a methanol–water supply and an evaporator/superheater unit. Before entering the reactor tube (inlet temperature T_{in}: 280°C) the liquid methanol–water mixture (1 mol CH_3OH/1.5 mol H_2O) was fed from the storage tank into the evaporator by a piston membrane metering pump (LEWA metering pump type EK — horizontal with worm gear and flange motor). After evaporation, the mixture was superheated to a temperature of 280°C. Two stainless steel tubes are arranged concentrically in each reactor tube. The heat needed for the endothermic reaction is provided by condensing steam ($p_{H_2O} = 65$ bar, $T_{H_2O} = 280$°C) that flows in the gap between the tubes. A copper coating is applied to the inner tube wall in order to avoid a Fischer–Tropsch reaction of the gas with the stainless steel. The inner tube is filled with a Cu–ZnO/Al_2O_3 type catalyst (Cat A, Cat B).

For the experiments discussed in this paper the four tubes were filled with different amounts and different kinds of catalyst (Cat A, Cat B). As an example of catalyst A the catalyst loadings of the four tubes were 10, 17, 25 and 50% of the reactor volume, so that for a reactor length of 1 m the catalyst beds have a length of 10, 17, 25 and 50 cm, respectively. Within the reactor tubes the heterogeneously catalyzed conversion into hydrogen, carbon dioxide and carbon monoxide takes place according to the following reactions [14]:

Steam reforming of methanol: $CH_3OH + H_2O \rightleftharpoons CO_2 + 3H_2$

Methanol decomposition: $CH_3OH \rightleftharpoons CO + 2H_2$

Water–gas shift reaction: $CO + H_2O \rightleftharpoons CO_2 + H_2$

In order to observe the dynamic behaviour of the steam reformer, the gas composition of the product gas is determined by a mass spectrometer on line with time intervals of 25 s. The temperature is measured at the reactor tube inlet (T_{in}) and in the catalyst bed at the reactor outlet (T_{Cat}). The pressure of the heat carrier is controlled and the pressure in the reactor is measured in the inlet and outlet of the reactor tube. The gaseous components H_2, CO_2, CO and, if present, CH_4 are analyzed on a gas chromatograph (Hewlett Packard Series II 5890) equipped with a thermal conductivity detector. The evaluation of the experimental results is given in detail by Düsterwald et al. [14].

3. Stationary operation

Stationary experiments with the reformer offer important information about the catalyst performance and the long-time behaviour of the catalyst. From these results, design data for the CMR can be estimated.

As part of the Joule III project experiments were carried out for methanol steam reforming under the test conditions described above with a $Cu/ZnO/Al_2O_3$ type catalyst (Cat B). The catalyst loading amounts to 25%. Fig. 2 shows the performance of the methanol steam reforming catalyst at two different heat carrier temperatures, i.e., 260 and 280°C.

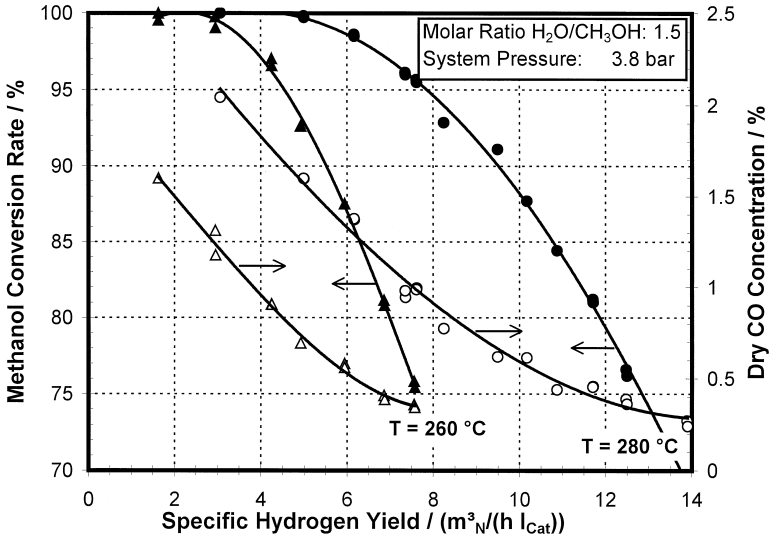

Fig. 2. Experimental reformer results for catalyst B [9].

The water–methanol ratio was chosen as 1.5 and the pressure was 3.8 bar. At a temperature of 260°C the conversion rate decreases from 100% at a yield of 3 m^3_N H_2/(h kg_{Cat}) to 75% at 7.5 m^3_N H_2/(h kg_{Cat}). The CO concentration decreases in this range from 1.5 to about 0.5% in the dry state. Raising the temperature up to 280°C leads to higher hydrogen yields at constant conversion rate. Again, the CO concentration decreases with decreasing methanol conversion, leading to high CO concentrations in the partial load regime. The design data for the compact reformer were determined from these experimental data as follows: assuming a heat carrier temperature of 280°C up to 95% of the methanol should be converted at full load. Under these conditions, the specific hydrogen yield is 8 m^3_N H_2/(h kg_{Cat}) at a CO content of 0.9% (dry state). These values lead to a power density of 12.5 kW electricity/l_{Cat}.

The specific production of hydrogen under constant experimental conditions can be taken as a yardstick of catalyst activity. This activity was analyzed as a function of operation time in the four reactor tubes within a period of 700 h. Fig. 3 shows the specific hydrogen production of the four reactor tubes as a function of the operation time. The loss in activity with operation time is most pronounced in the first catalyst zone (10% of the catalyst bed, Cat A), whereas almost no deactivation was observed with the catalyst filling of 50% of the reactor. Due to the practically linear decrease of activity with time the negative slope of these curves can be interpreted as a deactivation rate. From the experimental data a loss of active catalyst mass of 5.5 mg/h can be derived. This value is the same for all four tubes. The ageing process can be understood assuming that an active zone moves through the catalyst bed. Taking the ageing rates of the specific hydrogen production from the slope of the graphs in Fig. 3, the lifetime of a given mass of catalyst (Cat A) can be determined. Table 1 shows the time an amount of catalyst can be used until the rate of hydrogen production has decreased to 80% of the original value. Considering the data of tube 4, an operation time of nearly 4000 h can be achieved. This would be sufficient for an automobile application. These degradation rates were experimentally proved by experiments with 6000 h of catalyst lifetime and an operation time of 2700 h by Düsterwald [13].

4. Dynamic operation results

In addition to the stationary operation experiments the dynamic behaviour of the steam reformer provides impor-

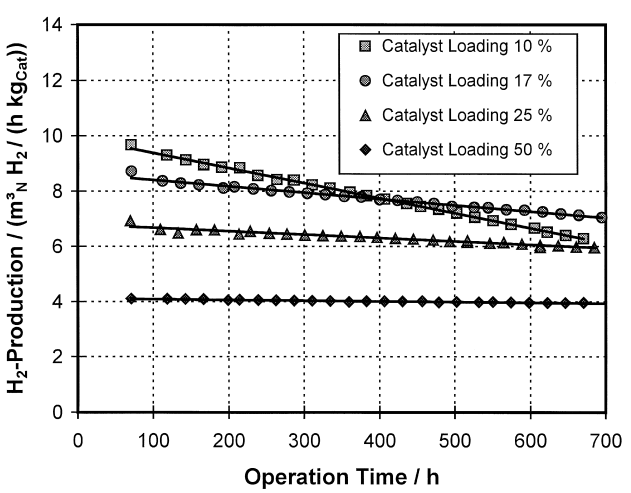

Fig. 3. Specific hydrogen production for different catalyst loadings (10, 17, 25, and 50%) as a function of operation time; catalyst A; molar water–methanol ratio 1.5:1; mixture density 0.905 kg/l (25°C); temperature of heating fluid 280°C; operating pressure 3.8 bar; methanol feed flow 3.8 mol/h each tube [14].

Table 1
Calculated operating time of the catalyst bed (Cat A) as a function of catalyst bed length for a hydrogen production decreased to 80% of the original value (source: Düsterwald et al. [14])

Tube	Catalyst bed length/cm	Operation time (80%)/h
1	10	431
2	17	656
3	25	1173
4	50	3864

tant information for use in a mobile system. The requirements for such a reformer are much more complex than for a usual chemical reactor, especially in the partial load regime.

In order to determine the dynamic behaviour of the steam reformer system the transient behaviour of the reactor after a load increase was investigated. This was realized by an abrupt electrical signal given to the pump leading to an increase of the liquid flow into the evaporator. Fig. 4 shows the response of the system related to the reformer off-gas flow as a function of the non-dimensional quantity t/τ, i.e., the ratio of the actual time to the residence time (8.5 s) of the gas in the system. The experimental results are given by the circles and triangles. As can be seen, the reformer off-gas flow increases only slightly during an initial period of 0.4τ, but then rises suddenly reaching 80% of the stationary flow at 1.5, i.e., a time period of 13 s. The load change is completed up to $>90\%$ after 25 s. In order to fulfil the requirements of a fuel cell drive in a passenger car the system should deliver 30% of the actual demand after 0.2 s. Since these high requirements for the dynamic behaviour cannot be satisfied by the current steam reformer an additional gas storage system for hydrogen is considered. An analysis of the processes of pumping, evaporating and reforming shows that the methanol–water pump causes the poorest response behaviour. In a real mobile application this time would be shorter due to a compact fuel injection system.

A further aspect of the dynamic performance of a steam reformer is the composition of the product gas during load changes. Fig. 5 shows the response function of the CO concentration after a load change from 2/3 to full capacity. This behaviour can also be observed after a load change from full capacity down to 2/3 partial load. As can be seen the CO concentration in the reformer off-gas changes very slowly. A stationary state is reached in 5–6 min, while the educt flow of the methanol–water mixture changes in just 25 s, indicated by the pump response function. The hydrogen product flow varies immediately with the educt flow. These experiments clearly indicate that the processes of hydrogen and carbon monoxide production occur on different time scales. The main reaction path for reforming methanol–water into hydrogen cannot include carbon monoxide as an intermediate product. This conclusion agrees with experiments of a different kind by Jiang et al. [15].

In order to support the experimental work for methanol steam reformers and to obtain a better insight into the interactions in a fuel cell drive system the reformer performance has been calculated by a simulation program. Operating strategies as well as control and regulating mecha-

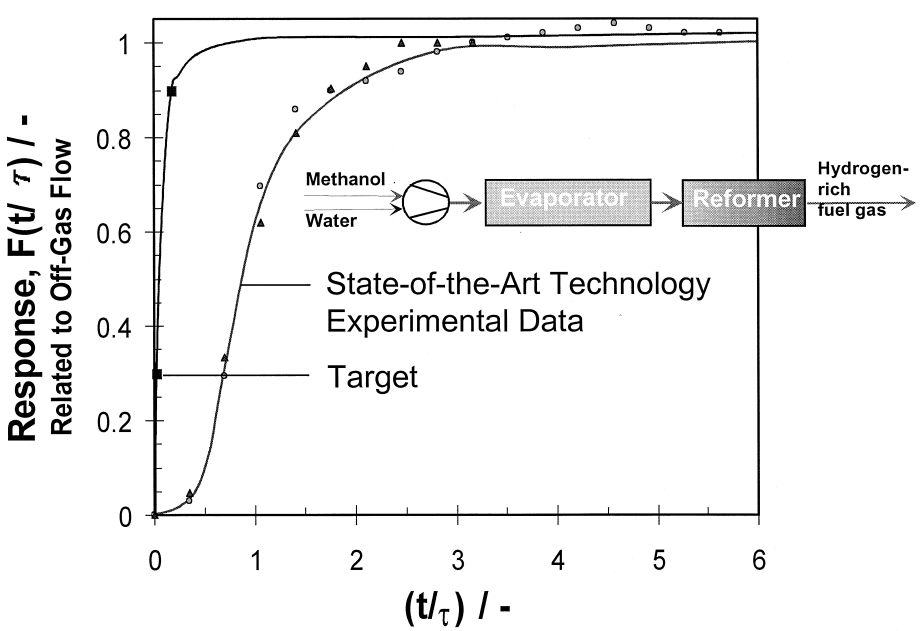

Fig. 4. Dynamic behaviour of the steam reformer system including evaporator and pump at 280°C and 3.8 bar (approximately from 2/3 to full capacity of the reactor; catalyst A; source: Düsterwald [13]).

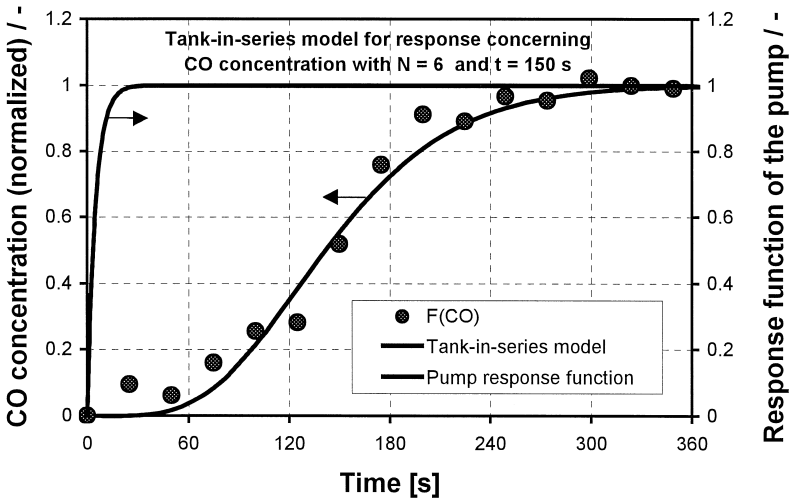

Fig. 5. Dynamic behaviour of the steam reformer system concerning CO concentration at 280°C and 3.8 bar (approximately from 2/3 to full capacity of the reactor; catalyst A; source: Düsterwald [13]).

nisms for a CMR, the gas treatment modules and the fuel cell can be developed in a driving cycle by means of simulation calculations.

The basis for simulations is characteristic data of all components of a fuel cell drive system. Vehicle data are taken, for example, from a VW Golf Citystromer. On the basis of vehicle requirements such as accelerating power (0–100 km/h in < 20 s) or maximum speed (120 km/h), it is possible to design the power classes for the individual components. The power output of the fuel cell should be at least 50 kW to fulfil these conditions. For the reformer, 7.31 kg of catalyst A is evaluated under the reaction conditions of 280°C and 20 bar. In the reformer, a thermal power of 110 kW (LHV H_2) is produced in four units with 29 tubes each. The four units are to be connected separately as a function of the partial load. More details about the simulation calculations are given by Düsterwald [13] and Peters et al. [16]. The requirements to be met by the individual system components are defined by the speed profile in the NEDC (or ECEEUDC) (see Fig. 6).

Fig. 7 shows the specific hydrogen production and the CO content at the reformer exit during simulation of the fuel cell drive system in the driving cycle. It can be seen that the reformer produces a maximum of 5.5 m^3_N H_2/(h kg_{Cat}) in the driving cycle. Although the reformer is activated in four units and the catalyst load is thus smoothed over time, the active reaction tubes are mostly operated in the partial load range. Considering the calculated hydrogen production during the driving cycle, it is obvious that the production rate of the reformer does not only directly depend on the velocity. As can be seen the hydrogen production does not abruptly go down to zero at stops and

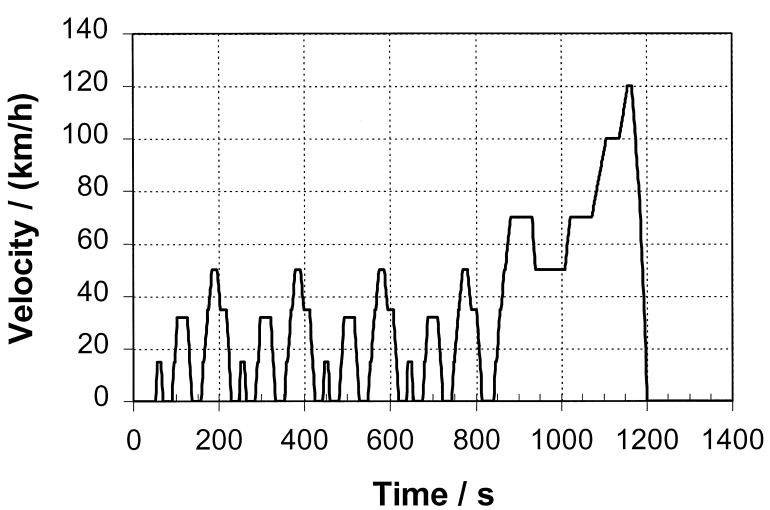

Fig. 6. New European Driving Cycle (NEDC or ECEEUDC).

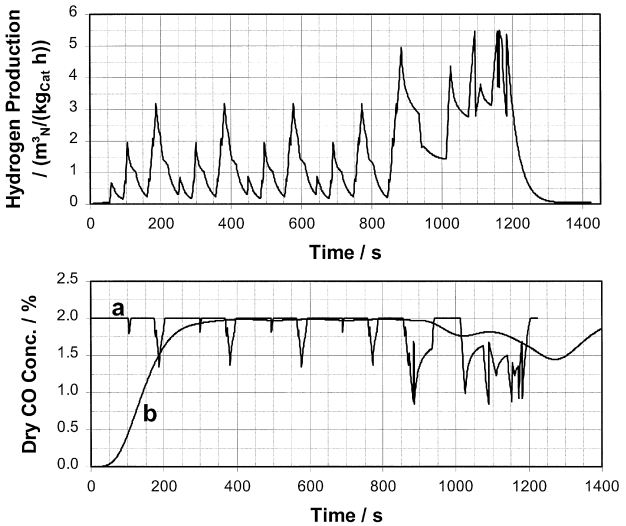

Fig. 7. Hydrogen production and CO concentration during the new European driving cycle; (a) simulation ignoring the response function of CO production [13,16]; (b) simulation considering the response function of CO production (Fig. 5).

at the end of the driving cycle. This behaviour is caused by the dynamic properties of the gas generation system.

Since the current hydrogen production system could not satisfy the actual demands of a fuel cell drive system an additional gas storage system has to be foreseen. If there is not enough hydrogen available from the gas cleaning system (Pd-membrane [11]), hydrogen is taken from a storage vessel. Otherwise, excess hydrogen will be compressed by a two-stage hydrogen compressor and stored again in the vessel. In order to control the hydrogen production, it is therefore necessary to scan both the actual requirement of the fuel cell and the charging level of the gas storage system. More details about control strategies are given in Ref. [13,16].

Fig. 7 also shows the CO concentration of the product gas during the driving cycle. Curve (a) was obtained ignoring the time behaviour of the CO concentration discussed in Fig. 5. The CO concentration at the reformer exit corresponds to the equilibrium value at partial load. Considering higher loads the CO content in the reformer off-gas decreases down to 1%. This approach must be chosen due to severe limitations of the calculation program [13]. With the actual simulation program MATLAB/SIMULINK the response function of the product gas quality can be considered, too. The CO concentration of the product gas is totally different (see curve (b)). At partial load the CO concentration also corresponds to the equilibrium value of 2.0% carbon monoxide. At the end of the driving cycle a minimum can be seen, i.e., 1.5% CO, obviously caused by the high methanol load in the extra urban cycle 5 min before this minimum appears. This transient behaviour is smoother compared to the results ignoring the experimental response function. Although the most important information about the dynamic properties of the reformer is included in the simulations the calculated time behaviour is faulty. The CO concentration is low at the beginning and increases slowly during the start-up phase of the reformer. This is in contradiction to experimental observations of the reformer start-up.

5. Starting up the steam reformer

Fig. 8 shows the concentrations of the different species, i.e., H_2, CO_2, CO, H_2O, CH_4, CH_3OH and DME during start-up. The start-up behaviour can be separated into three different phases. In the first phase (0–10 min) just hydrogen and water (12 l_N/h) leave the reactor through the measuring line of the mass spectrometer. Since no carbon dioxide or carbon monoxide is formed, it can be concluded that this hydrogen is not formed in the reforming reaction, but comes from purging. The long dead time is caused by the fact that the catalyst and the evaporating tube were previously purged with hydrogen at 280°C and 3.8 bar. The delivery lines to the evaporator are only filled with purge gas prior to start-up and must therefore be filled again with liquid educt. Eight minutes after switching on the pumps, the methanol–water mixture passes into the evaporating zone and abruptly evaporates. Two seconds later product gas leaves the reactor suddenly. Phase 2 begins.

In the second phase (10–18 min after start-up) the catalytic reaction starts and hydrogen is formed in the reforming reaction. This is indicated by the simultaneous formation of the carbon oxides, i.e., CO_2 and CO. The concentration of carbon monoxide in the product gas is of special interest especially for the gas treatment unit. As can be seen a maximum of up to 5% CO occurs. The steady-state equilibrium of 0.4% CO is then reached almost abruptly after 18 min. The H_2 content remains

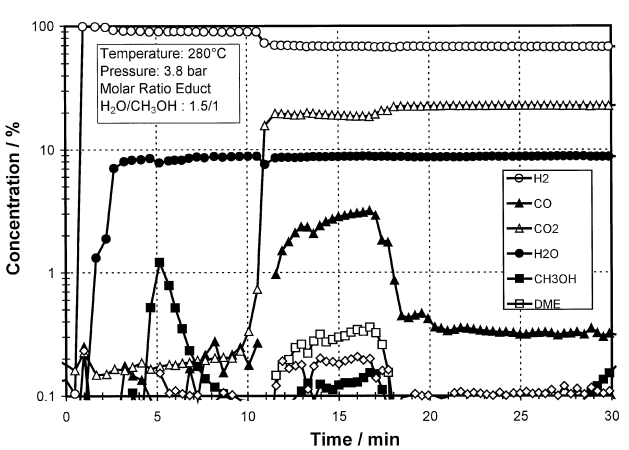

Fig. 8. Product concentration during start-up (from 0 to 3.8 mol CH_3OH/h); catalyst loading 50%; catalyst A; molar water–methanol ratio 1.5:1; mixture density 0.905 kg/l (25°C); temperature of heating fluid 280°C; operating pressure 3.8 bar.

almost constant at 67% during this phase. It is striking to note that the sum of carbon dioxide and carbon monoxide concentrations in the start-up phase is also almost constant. Only the ratio of CO to CO_2 changes dramatically. Such processes are not observed during load changes. The reasons for these observations are a further subject of investigations.

There exist different kinds of explanation for this behaviour [17–19]. Some scientists attribute the effect to the oxidation of active zones on the catalyst surface by a reduction of carbon dioxide to carbon monoxide. The species which is oxidized has been discussed controversial. The formation of DME during start-up leads to a lack of water on the adsorption sites of the alumina carrier (Al_2O_3). Figoli et al. [20] have shown that DME is formed in a side reaction from methanol at Al_2O_3 in the absence of water. Normally, water blocks these adsorption sites. This could be a hint that water is also absent on the active Cu adsorption sites and hydrogen is formed by the decomposition mechanism.

6. Conclusion

Experiments with a model of the later reactor design were performed to obtain data for a CMR. The hydrogen production of such a steam reformer was determined to be 10 m^3 $H_2/(h\ l_{Cat})$. This means that for 1 kW electrical power at the fuel cell 80 ml of reforming catalyst are necessary.

The catalyst shows linear catalyst ageing. A loss of 5.5 mg active catalyst mass/h was derived from the experimental data. An extrapolated operation time of 4000 h with a hydrogen production higher than 80% of the original performance was proved by over 2700 h of operation. Using these values, it was possible to design a CMR suitable for mobile application.

Investigations of the dynamic behaviour of the reformer led to response functions of the reformer system concerning its hydrogen production and the CO content of the product gas. These results were integrated into simulations regarding the new European driving cycle.

Discrepancies between the results of the experiments and the simulation especially during the start-up of the reformer show that theoretical and experimental work on this complex system have to be carried out together. A better understanding of the reforming process should lead to an improved reactor design fulfilling the requirements of a mobile application.

Acknowledgements

The authors would like to thank H. Kraut, H.-G. Düsterwald, P. Kuck and A. Eichhorn for carrying out the experimental works.

References

[1] R.A. Lemons, J. Power Sources 29 (1990) 251–264.
[2] Gas Research Institute, Light Duty Vehicle Full Fuel Emissions Analysis, Gas Research Institute, National Gas Vehicles Products Group, GRI-93/0472, 1994.
[3] NRC, Rethinking The Ozone Problem In Urban And Regional Air Pollution, National Academy Press, Washington, DC, 1991.
[4] B. Höhlein, P. Biedermann, D. Klemp, H. Geiß, Monogr. Forschungszent. Jülich 26 (1996) Forschungszentrum Jülich, Jülich.
[5] Daimler Benz, Booklet: NECAR II — Fahren ohne Emissionen, 1996.
[6] Daimler Benz, Booklet: NECAR III — mit Methanol in die Zukunft, 1997.
[7] B. Höhlein, P. Biedermann, Th. Grube, R. Menzer, J. Power Sources (1998) in press.
[8] R. Peters, B. Emonts, K.A. Friedrich, B. Höhlein, V.M. Schmidt, U. Stimming, Proc. World Car Conf., Riverside, CA, 1997, pp. 407–420.
[9] B. Emonts, J. Bøgild Hansen, S. Lægsgaard Jørgensen, B. Höhlein, R. Peters, J. Power Sources 71 (1998) 288–293.
[10] B. Ganser, PhD Thesis, RWTH Aachen, 1993.
[11] G. Colsmann, PhD Thesis, RWTH Aachen, 1995.
[12] B. Höhlein, M. Boe, J. Bøgild Hansen, P. Bröckerhoff, G. Colsman, B. Emonts, R. Menzer, E. Riedel, J. Power Sources 61 (1996) 143.
[13] H.-G. Düsterwald, PhD Thesis, RWTH Aachen, 1997.
[14] H.-G. Düsterwald, B. Höhlein, H. Kraut, J. Meusinger, R. Peters, U. Stimming, Chem. Eng. Technol. 9 (1997) 617–623.
[15] C.J. Jiang, D.L. Trimm, M.S. Wainwright, Appl. Catal., A 93 (1993) 245–255.
[16] R. Peters, H.-G. Düsterwald, B. Höhlein, Proc. 31st ISATA, Düsseldorf, Vol. Clean Power Sources and Fuels, 1997, pp. 99–107.
[17] R.O. Idem, N.N. Bakhshi, Ind. Eng. Chem. Res. 33 (1994) 2056–2065.
[18] R.O. Idem, N.N. Bakhshi, Ind. Eng. Chem. Res. 34 (1995) 1548–1557.
[19] C.V. Ovesen, B.S. Clausen, J. Schiøtz, P. Stoltze, H. Topsøe, J.K. Nørskov, J. Catal. (1996).
[20] N.S. Figoli, S.A. Hillar, J.M. Parera, J. Catal. 20 (1971) 230.